# EarthArXiv Coversheet

**Markus Möller[1,*], Florian Beyer[1], Marvin Dierks[1], Peter Horney[2], Peter Baumann[3], Nikolai Svoboda[4], and Henning Gerstmann[5]**

[*]corresponding author: Markus Möller (markus.moeller@julius-kuehn.de)
[1]Julius Kühn Institute (JKI) – Federal Research Centre for Cultivated Plants, Institute for Crop and Soil Science, Bundesallee 58, 38116 Braunschweig, Germany
[2]Julius Kühn Institute (JKI) – Federal Research Centre for Cultivated Plants, Institute for Strategies and Technology Assessment, Stahnsdorfer Damm 81, 14532 Kleinmachnow, Germany
[3]rasdaman GmbH, Hans-Hermann-Sieling-Str. 17, 28759 Bremen, Germany
[5]Leibniz Centre for Agricultural Landscape Research (ZALF), Research Data Management, Eberswalder Str. 84, 15374 Müncheberg
[5]Federal Agency for Nature Conservation (BfN), Alte Messe 6, 04103 Leipzig

## Peer-review statement

This manuscript is in review at Scientific Data and is **not** peer-reviewed.

# Germany-wide time series of interpolated phenological observations of main crop types between 1993 and 2021

**Markus Möller[1,*], Florian Beyer[1], Marvin Dierks[1], Peter Horney[2], Peter Baumann[3], Nikolai Svoboda[4], and Henning Gerstmann[5]**

[*]corresponding author: Markus Möller (markus.moeller@julius-kuehn.de)
[1]Julius Kühn Institute (JKI) – Federal Research Centre for Cultivated Plants, Institute for Crop and Soil Science, Bundesallee 58, 38116 Braunschweig, Germany
[2]Julius Kühn Institute (JKI) – Federal Research Centre for Cultivated Plants, Institute for Strategies and Technology Assessment, Stahnsdorfer Damm 81, 14532 Kleinmachnow, Germany
[3]rasdaman GmbH, Hans-Hermann-Sieling-Str. 17, 28759 Bremen, Germany
[5]Leibniz Centre for Agricultural Landscape Research (ZALF), Research Data Management, Eberswalder Str. 84, 15374 Müncheberg
[5]Federal Agency for Nature Conservation (BfN), Alte Messe 6, 04103 Leipzig

## ABSTRACT

The data descriptor represents a Germany-wide and spatio-temporally consistent $1 \times 1\,\mathrm{km}^2$ analysis-ready time series of interpolated days of the year (DOYs). The data set covers 56 entry dates of phenological development stages of 9 main crop types for the period between 1993 and 2021. The derivation of the 1624 records is based on phenological observations provided by German Meteorological Service (DWD) and the PHASE model, which combines the concept of growing degree days (GDD) with a geostatistical interpolation procedure. Each data set is characterized by the global accuracy metrics $R^2$ and $RMSE$. The data are stored as datacubes in the rasdaman Array DBMS which also serves to offer it via APIs based on the open OGC standards. A main application of the resulting data set is the extraction of phenological windows for any available year and user-defined region. This information is relevant for agricultural applications such as weather or biodiversity index derivation, crop-type classification, soil erosion, crop yield modeling or integrated pest management.

## Background & Summary

Plant phenological stages represent annual and periodically recurring plant physiological events or plant developmental stages[1]. Monitoring of phenological events has a long tradition and is carried out in different regions worldwide[2,3]. The German Meteorological Service (DWD) has maintained a nationwide monitoring program for decades, with about 1200 volunteer observers reporting the entry dates of about 160 phenological growth stages (≡ phases) in a standardized form[4] based on the internationally accepted BBCH scale (Table 1)[5]. The direct inter- and intra-annual use of the observations for the entire German territory is associated with several challenges:

- Before the reunification of the two German states, two separate observation programs were maintained. Since 1992, the two German phenological observation programs have been unified. This means that there are no observations for eastern Germany before 1992 (Figure 1a and b). In addition, due to changes in the observation program, not all classes have been continuously observed. This concerns, for example, phases 22 and 23 of winter wheat, whose monitoring was discontinued in 1992, or oat, where the observation program was interrupted between 1992 and 2014 (Figure 1c and d). While continuous observations between 1992 and today are available for winter wheat, this is not the case for oat. Therefore, the oat phases are not part of the data set presented here.
- The phenological observation network of the DWD belongs to the oldest European volunteered geographical information (VGI) programs[4]. Although the observations of the annual reporters go through a quality control process[4], phenological VGI are often associated with inconsistencies in terms of environmental conditions, geographic location, or timing of observations[7,8].
- For the practical use of the observations, the distances between the actual observation site and the respective study area

| Phase name | PHASE ID (DWD) | BBCH ID |
|---|---|---|
| Greenup | 1 | – |
| Beginning of flowering | 5 | 61 |
| Full flowering | 6 | 65 |
| End of flowering | 7 | 69 |
| Beginning of sowing | 10 | 0 |
| Emergence | 12 | 10 |
| Closed stand | 13 | 35 |
| $4^{th}$ leaf unfolded | 14 | 14 |
| Beginning of shooting/stem elongation | 15/67 | 31 |
| Beginning of leaf formation | 16 | 12 |
| Beginning of bud formation | 17 | 50 |
| Beginning of heading/tassel emergence | 18/66 | 51 |
| Beginning of milk ripening | 19 | 75 |
| Early dough ripening | 20 | 83 |
| Beginning of yellow ripening | 21 | 87 |
| Beginning of full ripening | 22 | – |
| Harvest | 24 | – |
| $1^{st}$ cut for hay | 25 | – |
| $1^{st}$ cut for silage | 26 | – |
| Tip of tassel emergence | 65 | 53 |

**Table 1.** Names and identifiers of DWD phenological phases[6] and corresponding BBCH equivalents[5].

must be taken into account[9]. This is complicated by the fact that the observations are characterized by both spatial variability and spatio-temporal gaps[10].

To improve the spatio-temporal availability of phenological information, the PHASE model was introduced[12]. The model couples the Growing Degree Days (GDD) concept with a geostatistical interpolation procedure. Based on the PHASE model, the data descriptor represents a Germany-wide and spatio-temporally consistent $1 \times 1$ km$^2$ analysis-ready time series (ARTS) of interpolated Day(s) of the Year (DOY) covering the potential entry date of phenological development stages (phases) of 9 main crop types for the period between 1993 and 2021. In total, there are 56 phases or three to nine different phases depending on the specific crop type.

A main application of the resulting data set is the extraction of phenological windows for any available year and user-defined region[13]. This information is relevant for applications such as agricultural weather or biodiversity index derivation, crop-type classification, soil erosion, crop yield modeling or integrated pest management[10,14–21].

The dataset is published and citeable via Digital Object Identifier (DOI)[22] following the FAIR principles to improve the findability, accessibility, interoperability, and reuse of digital (geo)data[23,24]. Furthermore, the data publication is linked to a Web Coverage Service (WCS) enabling a standardized web-based retrieval and analysis of spatio-temporal geospatial information[25,26] (see Data Records section). Finally, the used algorithms are documented in a software repository to make the life cycle of the data sets reproducible[27] (see Code Availability section).

# Methods

## PHASE model

The PHASE model represents a collection of **R** scripts[28]. Figure 2 shows the corresponding process chain of individual functions, which can be divided into the three groups (a) input data preparation, (b) temperature summation and (c) interpolation. Using the example of the phenological phase *heading* (phase ID = 18) of winter wheat (plant ID = 202) for the vegetation period 1999/2000, the most important steps of the process chain are described in the following sections. Compared to the original PHASE model[12], some modifications have been made in the current variant:

- GDDs are defined as the sum of daily mean temperature above a crop-specific base temperature[29,30]. The PHASE model calculates GDDs for each year, phase and location. The resulting phase- and year-specific distribution is subjected to a statistical filtering operation, which aims at the detection of observation inconsistencies. In this way, the model fit can be improved significantly, but the number of samples is thereby reduced considerably[12]. This fact is significant because the

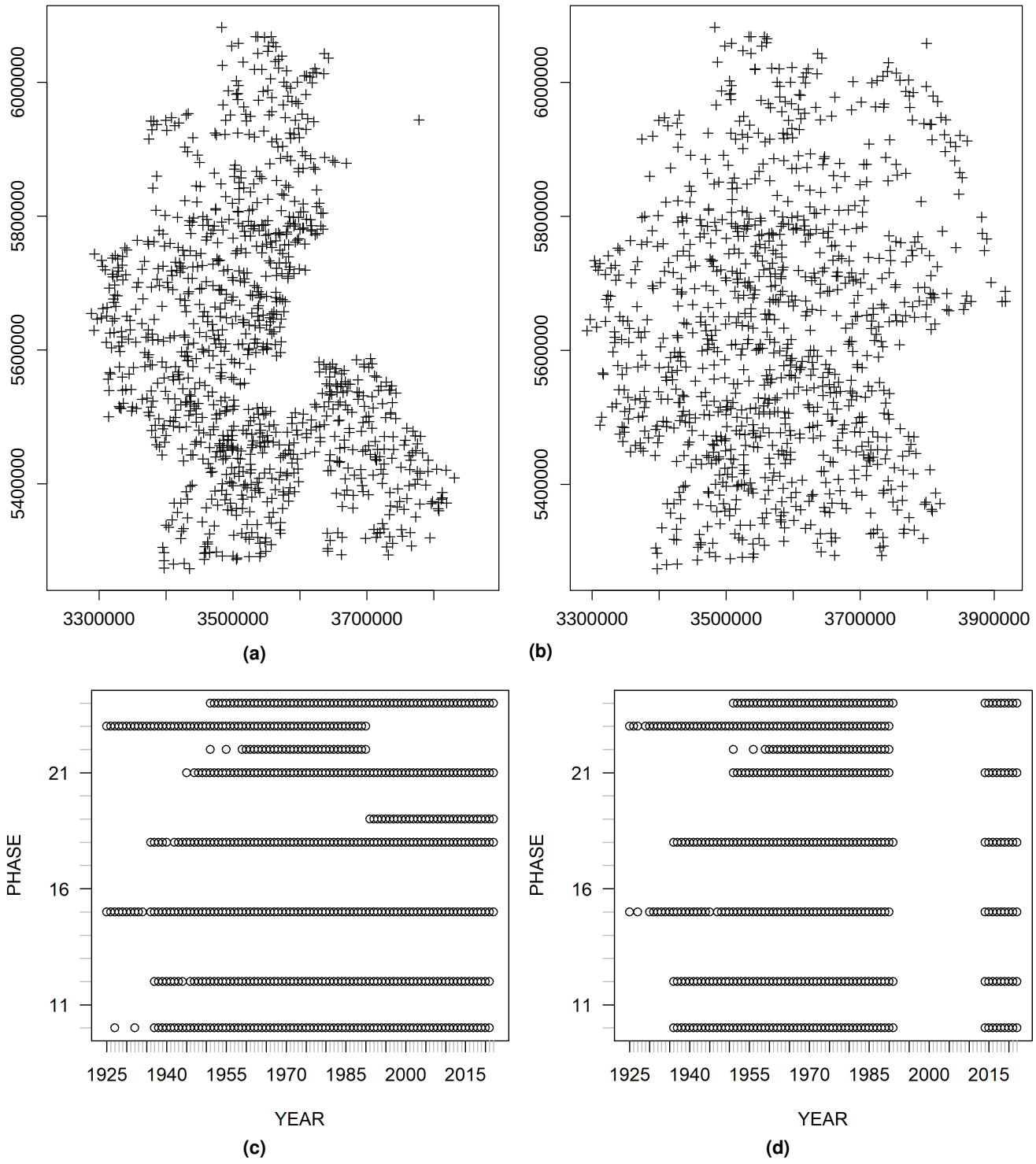


**Figure 1.** Spatial coverage of observations using the example of the winter wheat phase *heading* (Phase 18) for 1992 (a) and 2000 (b) as well as yearly temporal observation coverage of phenological phases for winter wheat (c) and oat (d; Table 1).

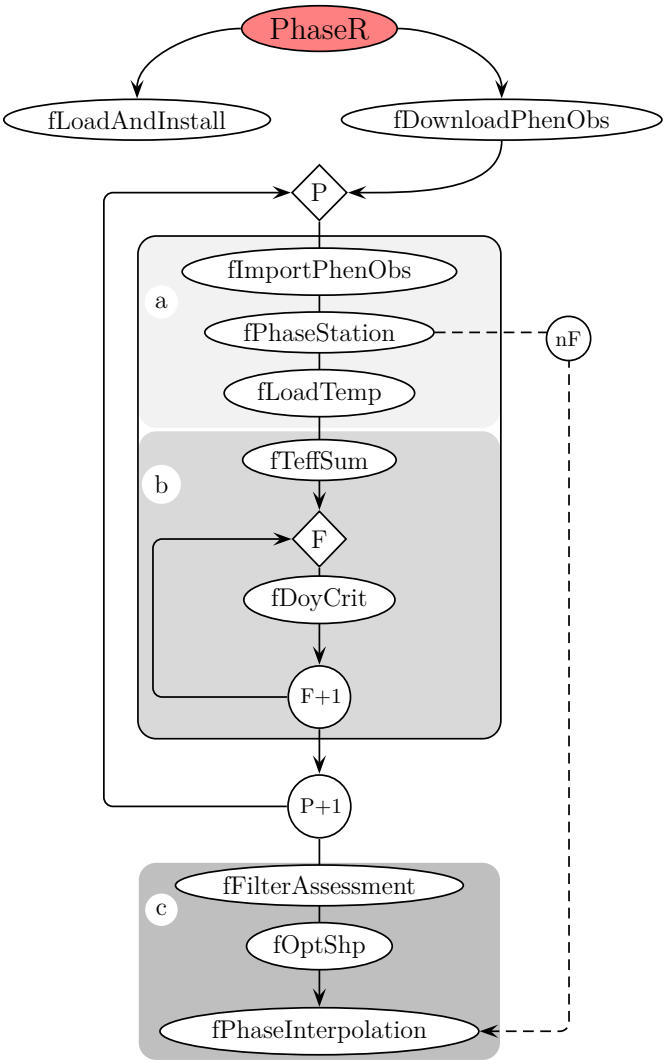


**Figure 2.** PHASE model process chain: relations between functions for the derivation of year- and plant-specific phenological phases[11] (P – Phases, F – standard deviation interval filter, nF – no Filter).

number of observations has drastically reduced over the years. Figure 3 illustrates the situation using the example of phenological observations for winter wheat, which have decreased between 1993 and 2021 to one quarter of the 1993 sample number. Hence, the modification aims at a trade-off between sample number and model fit (see Methods section).

- The original PHASE version uses a *Regression Kriging* variant[31] as the interpolation method, with a digital elevation model (DEM) serving as an additional explanatory variable. However, as the number of observations has decreased by both the applied filtering operation as well as by fewer reports over the years, the number of samples is often too small to derive reliable variograms. As a consequence, a spline algorithm was applied for the actual interpolation of phase-specific DOYs, which allows spatial forecasting models with a smaller number of samples[32] (see Methods section).

***Input data preparation***

After activating all necessary packages (function `fLoadAndInstall`), the procedure starts with the download of all crop-specific phenological observations (function `fDownloadPhenObs`). Then, the downloaded observations are imported (function `fImportPhenObs`) and coupled with phenological stations (function `fPhaseStation`), which results in a point vector dataset of observed phase- and year-specific Germany-wide events (Figure 1). Each file contains station-specific start DOYs (column DOY_start), at which the crop-specific vegetation period begins (Table 2). The start DOY for summer crops can be set by user (default value e.g., $DOY = 1$). For winter crops, the start DOYs correspond to the DOYs of a user-defined phase of the previous year. Outliers are removed using the *interquartile range* (IQR) criterion[33]. In Table 2, start DOYs for winter wheat in the year 2000 are shown corresponding to the DOYs of phase *beginning of sowing* (Phase ID = 10) in 1999.

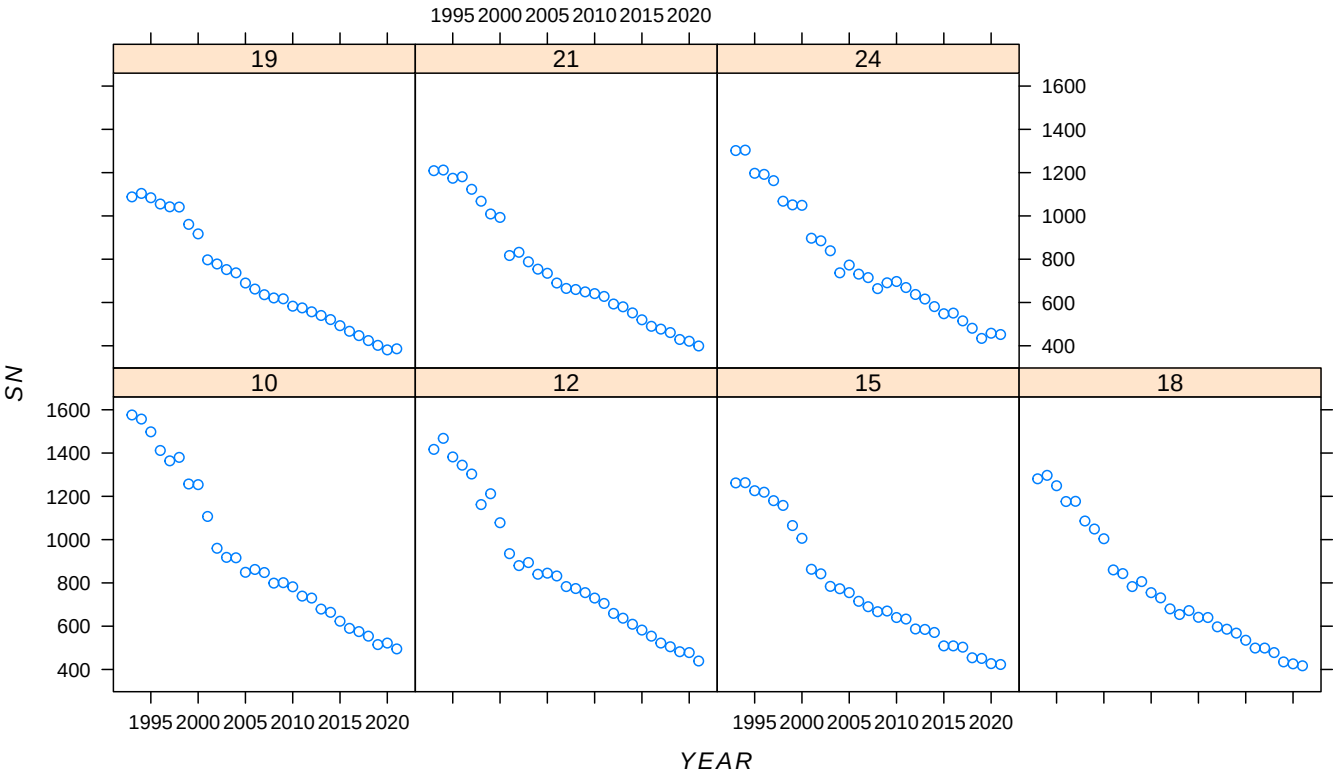


**Figure 3.** Relationships between unfiltered observation sample number (*SN*) and year for selected winter wheat phases.

The function `fLoadTemp` imports an interpolated temperature data set for a given vegetation period. The Germany-wide data set is provided by the DWD[34]. For this application, data of each single year are stored in csv format, which is related to a polygon vector dataset representing a Germany-wide weather grid of $1 \times 1$ km cell size.

For summer crops, the year-specific temperatures are incorporated. For winter crops, the temperatures of the previous year are also included, starting with the minimum Germany-wide observed DOY of the starting phase defined in the function `fPhaseStation`. In Table 3, an excerpt of an interpolated temperature data set is listed for the vegetation period of winter wheat in the year 2000. The very first DOY of the starting phase *beginning of sowing* (phase ID = 10) was observed on 19 August 1999 ($DOY = 231$), which results in the DOY difference $231 - 365 = -134$ and the corresponding temperatures.

***Temperature summation***

For a given growing season and phase, the function `fTeffSum` couples the phenological observations (Table 2) and the daily mean temperatures ($T$; Table 3). While a vegetation period of summer crops only considers the year of interest, a vegetation period of winter crops starts in the previous year on the DOYs of sowing. According to the equation (1), the plant-specific base temperatures ($T_B$) are subtracted during temperature summation, negative temperatures are deleted, and the remaining temperature values are weighted by a daylength factor ($DL$). For each phase- and year-specific station, the effective temperatures ($TS^{eff}$) are then accumulated (Table 4). Figure 4 displays a $TS^{eff}$ density plot for the phenological observations of the winter wheat phase *heading* in the year 2000.

$$TS^{eff} = \Sigma_{i=DOY_{start}}^{DOY_{obs}} \left( (T - T_B) \times \frac{DL_i}{24} \right) \tag{1}$$

The function `fDoyCrit` filters the phase- and year-specific distribution of effective temperature sums ($TS^{eff}$) in a two-stage procedure:

(1) Quantiles ($Q$) with user-defined probabilities $p$ of effective temperature sums ($TS^{eff}$) are calculated according to Equation (2). In Figure 4, the 0.5 quantile and the quantile value range for the probabilities variants $p \in [0.3, 0.7]$ are shown.

$$TS^{crit} = Q_p(TS^{eff}) \tag{2}$$

| STATION | ID | X | Y | GRID_ID | QL | YEAR | PLANT | PHASE | DATE | QF | DOY | DOY_start |
|---|---|---|---|---|---|---|---|---|---|---|---|---|
| 10725 | 268938 | 3396415 | 5273501 | 33965273 | 10 | 2000 | 202 | 18 | 20000511 | 1 | 131 | 291 |
| 10723 | 268976 | 3410415 | 5279501 | 34105279 | 10 | 2000 | 202 | 18 | 20000516 | 1 | 136 | 281 |
| 10768 | 269201 | 3426415 | 5280501 | 34265280 | 10 | 2000 | 202 | 18 | 20000608 | 1 | 159 | 275 |
| 10802 | 268105 | 3456415 | 5286501 | 34565286 | 10 | 2000 | 202 | 18 | 20000610 | 1 | 161 | 300 |
| 10700 | 268439 | 3505415 | 5288501 | 35055288 | 10 | 2000 | 202 | 18 | 20000528 | 1 | 148 | 295 |
| 10786 | 268538 | 3523415 | 5290501 | 35235290 | 10 | 2000 | 202 | 18 | 20000602 | 1 | 153 | 289 |
| … | … | … | … | … | … | … | … | … | … | … | … | … |

**Table 2.** Excerpt of an attribute table of year- and phase-specific phenological stations on example of the winter wheat phase *heading* (phase ID = 18) in the year 2000 (STATION – ID of a phenological observation station, ID – object ID, X/Y – coordinates, GRID_ID – raster cell ID related to a Germany-wide weather grid, QL – DWD quality level, YEAR – year of observation, PHASE – phase ID, PLANT – crop ID, DATE – date of a beginning phenological phase, QF – DWD quality flag, DOY – day of the year of a beginning phenological phase, DWD_start – day of the year on, which the crop-specific vegetation period begins).

| GRID_ID | T-134 | T-133 | T-132 | T-131 | T-130 | T-129 | T-128 | T-127 | T-126 | T-125 | T-124 | … |
|---|---|---|---|---|---|---|---|---|---|---|---|---|
| 32805658 | 152 | 157 | 143 | 136 | 165 | 203 | 250 | 204 | 186 | 180 | 183 | … |
| 32805661 | 153 | 158 | 144 | 137 | 166 | 204 | 250 | 205 | 186 | 181 | 183 | … |
| 32815657 | 153 | 157 | 144 | 137 | 165 | 203 | 250 | 204 | 186 | 181 | 183 | … |
| 32815658 | 152 | 157 | 143 | 136 | 165 | 203 | 250 | 204 | 186 | 180 | 183 | … |
| 32815659 | 152 | 157 | 144 | 137 | 165 | 203 | 250 | 204 | 186 | 181 | 183 | … |
| 32815660 | 153 | 157 | 144 | 137 | 165 | 203 | 250 | 205 | 186 | 181 | 183 | … |
| … | … | … | … | … | … | … | … | … | … | … | … | … |

**Table 3.** Excerpt of an interpolated temperature data set [°C × 10] for the vegetation period of winter wheat for the year 2000 (GRID_ID – raster cell ID related to a Germany-wide weather grid, T[1:365]: daily temperatures [°C × 10] of the year of harvest, T[-X:-1] (only for winter crops): daily temperatures [°C × 10] of the year of sowing (-X=DOY-365)).

| GRID_ID | LON | LAT | STATION | ID | YEAR | PLANT | PHASE | DATE | DOY | DOY_start | T_SUMS |
|---|---|---|---|---|---|---|---|---|---|---|---|
| 33965273 | 7,6311 | 47,5980 | 10725 | 1 | 2000 | 202 | 18 | 20000511 | 131 | -75 | 2409 |
| 34105279 | 7,8160 | 47,6540 | 10723 | 2 | 2000 | 202 | 18 | 20000516 | 136 | -85 | 2580 |
| 34265280 | 8,0288 | 47,6650 | 10768 | 3 | 2000 | 202 | 18 | 20000608 | 159 | -91 | 2545 |
| 34565286 | 8,4277 | 47,7216 | 10802 | 4 | 2000 | 202 | 18 | 20000610 | 161 | -66 | 4050 |
| 35055288 | 9,0810 | 47,7410 | 10700 | 5 | 2000 | 202 | 18 | 20000528 | 148 | -71 | 3208 |
| 35235290 | 9,3212 | 47,7586 | 10786 | 6 | 2000 | 202 | 18 | 20000602 | 153 | -77 | 3534 |
| … | … | … | … | … | … | … | … | … | … | … | … |

**Table 4.** Excerpt of an attribute table of station- and phase-specific temperature sums (TS=T_SUMS) on example of the winter wheat phase *heading* in the year 2000 (GRID_ID – raster cell ID related to a Germany-wide weather grid, LON/LAT – Longitude/Latitude, STATION – ID of a phenological observation station, YEAR – year of observation, PHASE – phase ID, PLANT – crop ID, DATE – date of a beginning phenological phase, DOY – day of the year of a beginning phenological phase, DOY_start – starting DOY, from which temperature sums are calculated, T_SUMS – phase- and station-specific temperature sums).

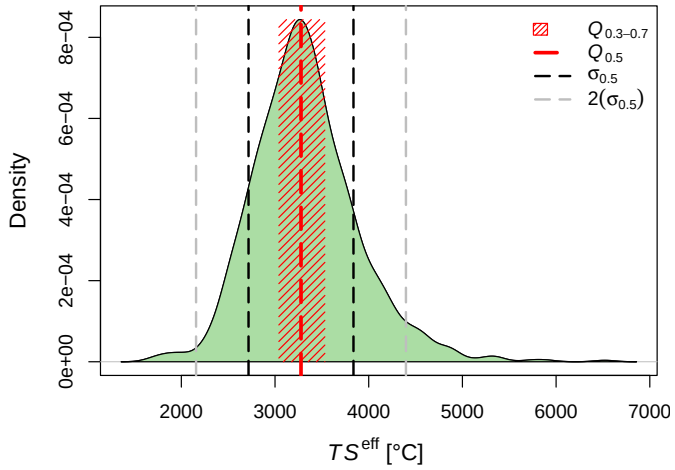


**Figure 4.** $TS^{eff}$ density plot of phenological observations for the winter wheat phase *heading* in the year 2000, corresponding quantiles with different probabilities ($Q_{0.3-0.7}$) as well as single ($\sigma$) and double standard derivations ($2(\sigma_{0.5})$) for $Q_{0.5}$.

(2) The resulting critical effective temperature sums ($TS^{crit}$) are used to determine the station- and phase-specific DOY ($DOY^{P}$) when the condition $TS^{eff} \geq TS^{crit}$ is fulfilled.

(3) The remaining $TS^{eff}$ distribution is statistically filtered using standard deviation variants resulting from multiplying the standard deviation ($\sigma$) and a user-defined factor ($STD$). Figure 4 shows the positions of the first ($\sigma_{0.5}$) and second standard deviation ($STD = 2 \Rightarrow 2(\sigma_{0.5})$) for the 0.5 quantile variant ($Q_{0.5}$).

#### *Interpolation and accuracy asessment*

For each filtering variant, $DOY^{P}$ and observed DOY values ($DOY^{obs}$) are compared by calculating the Pearson correlation coefficient ($COR$)[35], Root Mean Squared Error ($RMSE$)[36], and Mean Absolute Error ($MAE$)[37]. By applying the function `fFilterAssessment`, the optimal filtered observation variant ($O^{opt}$) results from the maximum value of the product of observation sample number ($SN$) and $COR$ value. Optionally, the $MAE$ value can also be taken into account (Eq. (3)). Table 5 contains the accuracy metrics and assessment result for all filtering variants of the winter wheat phase *heading* in the year 2000.

$$O^{opt} = \frac{SN \times COR}{(MAE)} \tag{3}$$

The most optimal variant is extracted by the function `fOptShp`, which corresponds in Table 5 to the 0.40 quantile ($Q_{0.40}$) with a standard deviation factor of $STD = 1.5$. The final interpolation of the resulting point data set is performed by applying a *regression kriging* or *thin plate spline algorithm*[38,39], respectively, using the winter wheat phase *heading* in 2000 as an example (function `fPhaseInterpolation`). Optionally, local accuracy metrics can be derived for each interpolation result, allowing characterization of thelocal prediction uncertainty of each grid cell[10].[10]. Here, the interpolation algorithms are associated with the local accuracy metrics *Kriging Standard Variance* ($KSV$) and *Spline Standard Error* ($SSE$), both of which represent the spatial standard error of estimation[39,40].

Figure 5 visualizes both interpolation variants as well as the corresponding local accuracy metrics. Finally, external global validation is performed in addition to the local accuracy assessment to provide an "indication of the limits of the predictions"[41] (see Technical Validation section).

## BonaRes repository

The BonaRes Repository (“Soil as a sustainable resource for the bioeconomy”) is a domain specific repository tailored to and basically open for soil and agricultural research data, but also for related domains, e.g. hydrological data or weather data typically in tabular (csv, xlsx) or in geodata formats (FeatureClass, KML, shapefile). The repository is designed as a Spatial Data Infrastructure (SDI), since the majority of data that is published originates from the landscape context and is therefore spatial data. Through this SDI, all data are managed and made available for reuse via download and Web Map Service (WMS) based on open and internationally adopted standards. The underlying concept of Research Data Management (RDM) follows the FAIR data principles for improving the findability, accessibility, interoperability and reusability of research data and is in

| Q | RMSE | MAE | SN | COR | YEAR | STD | PLANT | PHASE | OPT |
|---|---|---|---|---|---|---|---|---|---|
| 0.3 | 4.11 | 3.51 | 584 | 0.85 | 2000 | 1 | 202 | 18 | 494.84 |
| 0.35 | 3.99 | 3.39 | 589 | 0.85 | 2000 | 1 | 202 | 18 | 502.5 |
| 0.4 | 3.94 | 3.34 | 595 | 0.86 | 2000 | 1 | 202 | 18 | 509.13 |
| 0.45 | 4.05 | 3.38 | 602 | 0.85 | 2000 | 1 | 202 | 18 | 510.28 |
| 0.5 | 3.97 | 3.33 | 589 | 0.86 | 2000 | 1 | 202 | 18 | 503.78 |
| 0.55 | 4.14 | 3.5 | 589 | 0.84 | 2000 | 1 | 202 | 18 | 495.96 |
| 0.6 | 4.04 | 3.44 | 558 | 0.85 | 2000 | 1 | 202 | 18 | 476.61 |
| 0.65 | 4.17 | 3.57 | 543 | 0.85 | 2000 | 1 | 202 | 18 | 461.01 |
| 0.7 | 4.34 | 3.76 | 518 | 0.84 | 2000 | 1 | 202 | 18 | 434.65 |
| 0.3 | 5.48 | 4.63 | 736 | 0.74 | 2000 | 1.5 | 202 | 18 | 546.01 |
| 0.35 | 5.37 | 4.51 | 742 | 0.74 | 2000 | 1.5 | 202 | 18 | 551.22 |
| **0.4** | **5.37** | **4.49** | **749** | **0.74** | **2000** | **1.5** | **202** | **18** | **553.85** |
| 0.45 | 5.35 | 4.44 | 745 | 0.74 | 2000 | 1.5 | 202 | 18 | 552.78 |
| 0.5 | 5.31 | 4.42 | 735 | 0.75 | 2000 | 1.5 | 202 | 18 | 549.64 |
| 0.55 | 5.45 | 4.56 | 728 | 0.74 | 2000 | 1.5 | 202 | 18 | 537.79 |
| 0.6 | 5.46 | 4.6 | 711 | 0.75 | 2000 | 1.5 | 202 | 18 | 531.12 |
| 0.65 | 5.64 | 4.8 | 703 | 0.74 | 2000 | 1.5 | 202 | 18 | 522.15 |
| 0.7 | 5.9 | 5.09 | 691 | 0.73 | 2000 | 1.5 | 202 | 18 | 507.15 |
| 0.3 | 6.9 | 5.73 | 857 | 0.61 | 2000 | 2 | 202 | 18 | 518.68 |
| 0.35 | 6.77 | 5.58 | 861 | 0.61 | 2000 | 2 | 202 | 18 | 521.57 |
| 0.4 | 6.75 | 5.55 | 867 | 0.6 | 2000 | 2 | 202 | 18 | 521.25 |
| 0.45 | 6.88 | 5.62 | 877 | 0.59 | 2000 | 2 | 202 | 18 | 515.64 |
| 0.5 | 6.97 | 5.72 | 879 | 0.59 | 2000 | 2 | 202 | 18 | 515.91 |
| 0.55 | 7.14 | 5.9 | 879 | 0.58 | 2000 | 2 | 202 | 18 | 512.07 |
| 0.6 | 7.24 | 6.01 | 869 | 0.58 | 2000 | 2 | 202 | 18 | 506.45 |
| 0.65 | 7.29 | 6.12 | 851 | 0.6 | 2000 | 2 | 202 | 18 | 508.18 |
| 0.7 | 7.44 | 6.34 | 833 | 0.62 | 2000 | 2 | 202 | 18 | 512.5 |
| 0.3 | 8.02 | 6.52 | 925 | 0.51 | 2000 | 2.5 | 202 | 18 | 474.83 |
| 0.35 | 7.96 | 6.43 | 935 | 0.49 | 2000 | 2.5 | 202 | 18 | 462.67 |
| 0.4 | 7.91 | 6.38 | 940 | 0.49 | 2000 | 2.5 | 202 | 18 | 458.5 |
| 0.45 | 7.89 | 6.36 | 943 | 0.48 | 2000 | 2.5 | 202 | 18 | 457.31 |
| 0.5 | 7.98 | 6.45 | 945 | 0.48 | 2000 | 2.5 | 202 | 18 | 454.27 |
| 0.55 | 8.18 | 6.66 | 948 | 0.47 | 2000 | 2.5 | 202 | 18 | 447.24 |
| 0.6 | 8.34 | 6.84 | 946 | 0.47 | 2000 | 2.5 | 202 | 18 | 445.24 |
| 0.65 | 8.62 | 7.13 | 945 | 0.47 | 2000 | 2.5 | 202 | 18 | 439.93 |
| 0.7 | 8.87 | 7.43 | 936 | 0.47 | 2000 | 2.5 | 202 | 18 | 440.54 |
| 0.3 | 8.66 | 6.95 | 956 | 0.45 | 2000 | 3 | 202 | 18 | 433.22 |
| 0.35 | 8.49 | 6.79 | 960 | 0.45 | 2000 | 3 | 202 | 18 | 427.41 |
| 0.4 | 8.35 | 6.67 | 961 | 0.44 | 2000 | 3 | 202 | 18 | 426.99 |
| 0.45 | 8.36 | 6.67 | 965 | 0.44 | 2000 | 3 | 202 | 18 | 422.2 |
| 0.5 | 8.45 | 6.76 | 968 | 0.43 | 2000 | 3 | 202 | 18 | 415.84 |
| 0.55 | 8.61 | 6.96 | 970 | 0.42 | 2000 | 3 | 202 | 18 | 411.93 |
| 0.6 | 8.87 | 7.2 | 973 | 0.41 | 2000 | 3 | 202 | 18 | 402.22 |
| 0.65 | 9.08 | 7.45 | 970 | 0.42 | 2000 | 3 | 202 | 18 | 403.09 |
| 0.7 | 9.47 | 7.86 | 970 | 0.41 | 2000 | 3 | 202 | 18 | 401.62 |

**Table 5.** Accuracy metrics and assessment results for variants of quantiles and standard deviation filters on example of the winter wheat phase *heading* in the year 2000 (MAE – Mean Absolute Error, MSE – Mean Squared Error, COR – Pearson correlation coefficient. RMSE – Root Mean Squared Error, PLANT – crop ID, PHASE – phase ID, SN – observation sample number, STD – standard derivation factor, YEAR – year of observation, OPT – result of $COR \times SN$).

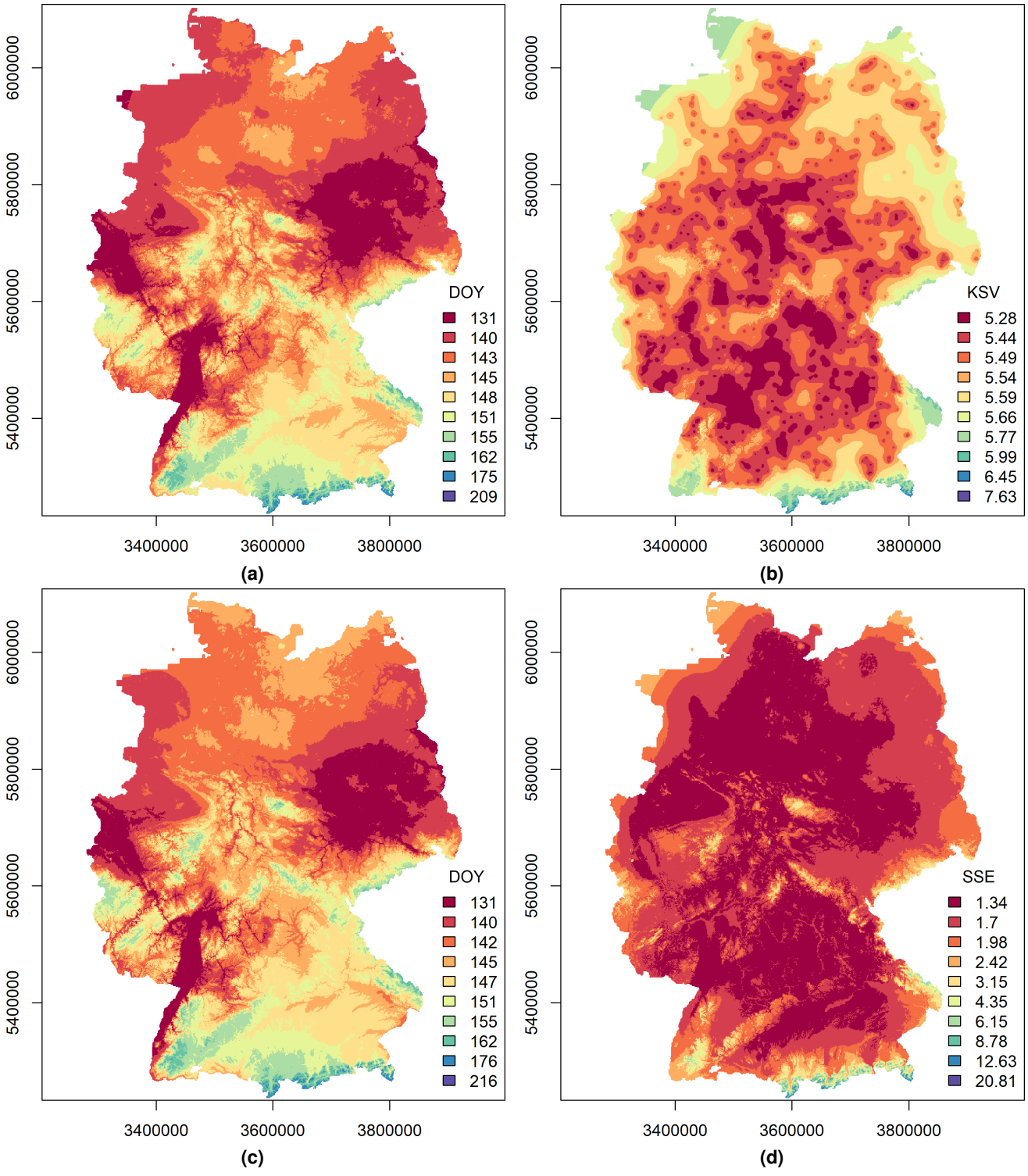


**Figure 5.** Interpolated DOYs based on *Regression Kriging* and *Thin Plate Spline* (a, c) as well as local accuracy metrics *Kriging Standard Variance* (KSV) and *TPS Standard Error* (SSE) (b, d) for the winter wheat phase *heading* in the year 2000.

| Phase ID | Crop ID | | | | | | | |
|---|---|---|---|---|---|---|---|---|
| | 201 | 202 | 203 | 204 | 205 | 208 | 215 | 252/253 |
| 1 | • | | | | | | | |
| 5 | | | • | | • | | • | |
| 6 | | | • | | | | | |
| 7 | | | | | | | | |
| 10 | | • | • | • | • | • | • | • |
| 12 | | • | • | • | • | • | • | • |
| 13 | | | | | | | | • |
| 14 | | | | | • | | | |
| 15 | | • | • | • | | • | | |
| 17 | | | | | • | | | |
| 18 | | • | • | • | | | | |
| 19 | | • | | | | • | • | |
| 20 | | | | | | | • | |
| 21 | | • | • | • | | • | • | |
| 22 | | | | | • | | | |
| 24 | | • | • | • | • | • | • | • |
| 25 | • | | | | | | | |
| 26 | • | | | | | | | |
| 65 | | | | | | | • | |
| 66 | | | | | | • | | |
| 67 | | | | | • | | • | |

**Table 6.** Interpolated Germany-wide phenological phases (see Table 1). 201 – permanent grassland | 202 – winter wheat | 203 – winter rye | 204 – winter barley | 205 – winter rape | 208 – summer oat | 215 – maize | 252/253 – fodder/sugar beet.

line with good scientific practice[23]. It is complemented by a comprehensive description with standardized metadata and DOI assignment[42].

The metadata schema combines all elements of DataCite[43] and INSPIRE[44], supplemented by detailed attribute metadata that facilitate scientific reuse. Metadata is captured in a user-friendly manner and entered via an online metadata editor, including thesauri (FAO: AGROVOC[45], EEA: GEMET[46]), licenses (Creative Commons[47]: Attribution 4.0 International (CC BY 4.0)), lineage elements, and data access points (SDI with OGC services such as spatial search and WMS for visualization).

The download formats provided in the BonaRes repository (GDB, TXT, CSV, XLSX) are oriented towards the needs of the target group and can be extended upon request (e.g. GeoJSON, KML, GML, GPX). Likewise, the currently offered target coordinate systems (EPSG: 25833, 31467, 31468, 4326) can be extended.

Data steward services include in-person support, metadata review, and tools for the entire workflow: Data submission, metadata description, and publication. Due to the broad diversity of soil and agricultural data, customized RDM strategies have been developed to improve data quality and make them easily citable.

The BonaRes approach to foster the reuse of published data in the agricultural domain is such that data are compiled into highly aggregated datasets that are useful for reuse. In addition, there is the opportunity to compile datasets into data collections (AGROVOC). Data collections consist of a parent dataset, which contains e.g. the geodata, and several child datasets. All datasets are semantically linked via metadata. In addition, it is possible to represent genuine relations (primary; foreign key) by means of the data model. The parent dataset is the gateway to the data collections and acts as a landing page for the DOI. For reuse and thus citation in scientific journals, this has the advantage of being able to cite various datasets with one DOI. Data collections are arbitrarily expandable. When a download request is submitted, all datasets subordinate to the DOI are initially provided, but can be selected.

# Data Records

## Repository data records

The PHASE data set is available for the entire area of Germany, covering three to nine phenological phases depending on the crop type (Table 6) and 29 years (1993–2021), resulting in 1624 records. The entire dataset is made available through the BonaRes repository[48] and contains the following files:

- The current crop-specific (PLANT) and year-specific (YEAR) Germany-wide interpolation products are stored as csv files with the naming convention `[PLANT]_[YEAR].csv`. Each file contains all year- and phase-specific DOYs (Table 6) and can be coupled to a Germany-wide weather grid via the column `GRID_ID`, which corresponds to DWD reference units[49] with a geometric resolution of $1 \times 1\,\mathrm{km}^2$. The weather grid can be downloaded from the PhaseR Github repository[11].

- Each phase- and year-specific interpolation result is characterized by global accuracy metrics. All crop-specific metrics are summarized in a file with the naming convention `VAM_[PLANT].csv`. Table 7 shows the accuracy metrics for the interpolated optimal phenological observation variants for winter wheat phase *heading* for the years 1993 to 2021.

- In addition to the interpolation results and accuracy metrics, the Germany-wide temperature input data are provided with the naming convention `tmit_[YEAR].csv`. The files do not include a header and contain year-specific gridded temperatures (columns 2-366). Data sets are provided by DWD[50] and can be coupled with DWD reference units[49] with a geometric resolution of $1 \times 1\,\mathrm{km}^2$ (column $1 \equiv$ `GRID_ID`) of the file `[PLANT]_[YEAR]. csv`).

### Coverages and Web Coverage (Processing) Services

While the BonaRes repository ensures data availability according to FAIR criteria[42], web services enables direct ARTS access[25]. For this purpose, data sets are imported into the PHASE Data Cube (see Usage Notes section). There, the data sets are managed locally and made available via the Open Geospatial Consortium (OGC) standard WCS[51]. We briefly introduce the coverage data and service model.

In ISO, OGC, and INSPIRE the concept of coverages is used to denote "fields" (as in physics) in general, and specifically serve to model multi-dimensional raster data in an encoding-independent manner; both regular and irregular spatio-temporal grids are supported. The central standard is the OGC Coverage Implementation Schema (CIS) which is identical to ISO 19123-2. A coverage data structure consists of four main components (1) the domain (Where are these data located in space and time?), (2) the range (the data values), (3) the range type (What is the structure of the range values and their meaning?) and (4) metadata (any additional information the coverage should carry along). Such coverages can be encoded in the common formats, such as GeoTIFF, NETCDF, or JSON.

Based on the coverage definition above, the WCS standard is defined. Unlike a WMS[52], which derives map images suitable for human consumption, a WCS allows extraction of spatio-temporal subsets – possibly processed on server side – as the original data, which can be interpreted, analyzed, and rendered using any programming language, browser, or geographic information system (GIS). The WCS of the PHASE Data Cube is documented in an OpenAPI specification[53]. An example of a WCS request extracting from winter wheat, together with the resulting entry dates of phenological stages, is shown in code example 1.

The associated metadata are also standardized and stored as part of the coverage object. This metadata record can be extended with any additional information[54] such as, in an INSPIRE setup, with INSPIRE-compliant metadata[55]. In the WCS code example 2, the metadata of the PHASE Data Cube are queried for winter wheat. The output snippet shows global accuracy measures as they are calculated and stored for all interpolations results (see Technical Validation section, Table 7).

One of the components of the modular WCS suite is the Web Coverage Processing Service (WCPS)[56,57], a geo datacube analytics language. It allows for server-side filtering, processing and fusion in a high-level, language-independent way. In our work, we heavily use WCPS as it gives high flexibility and is compact to use.

The rasdaman Array DBMS is both the OGC WCS reference implementation and INSPIRE WCS Good Practice. In this study, rasdaman is used to manage, server, and analyze all the datacubes (see Usage Note section).

**Code example 1.** WCS query for DOYs of all beginning phenological phases of winter wheat (see Table 6) as csv format for the year 2000 (coverage name: "PHASE_202_Winterweizen") and a location near Braunschweig (Germany).

```
https://datacube.julius-kuehn.de/flf/ows?&SERVICE=WCS&VERSION=2.0.1&REQUEST=GetCoverage&
    COVERAGEID=PHASE_202_Winterweizen&SUBSET=ansi("2000-01-01")&SUBSET=E(597930)&SUBSET=N
    (5795243)&FORMAT=text/csv

Output: "112.5206 142.4212 172.3821 198.0325 218.6161 275.6248 290.5179"
```

## Technical Validation

While the actual interpolation is performed using all filtered observations (see Methods section), the external validation is based on a random division into a training and a test data set of 75 % and 25 %, respectively, considering the target parameter

**Code example 2.** WCS query to recieve metadata for winter wheat phases (coverage name: "PHASE_202_Winterweizen").

```
https://datacube.julius-kuehn.de/flf/ows?&SERVICE=WCS&VERSION=2.0.1&REQUEST=DescribeCoverage
    &COVERAGEID=PHASE_202_Winterweizen

Output XML snipped:
...
    <record>
        <PLANT>202</PLANT>
        <PHASE>18</PHASE>
        <YEAR>2000</YEAR>
        <ON>747</ON>
        <MSE>26.1050033362502</MSE>
        <MAE>4.00605421643839</MAE>
        <RMSE>5.10930556301443</RMSE>
        <R2>0.394334005817017</R2>
    </record>
...
```

distribution. The similarity of the two distributions is tested by applying the nonparametric *Kolmogorov Smirnov* goodness-of-fit (KS) test[58].

Model building is based on the training data set. The test data set is used for validation[59] providing the metrics *MAE*[37], Mean Squared Error (*MSE*)[60], *RMSE*[36] and $R^2$[61]. Table 7 shows the global accuracy metrics for the winter wheat phase *heading* for the years 1993 to 2021.

Figure 6 summarizes the phase-specific accuracy metrics $R^2$ and *RMSE* for all interpolation results. In addition, interpolation results based on unfiltered phenological observations were produced (see Figure 2) to illustrate the impact of the filtering and optimization approach on modeling accuracy. Accordingly, the $R^2$ values of the early phases 10 and 12 are comparable for both categories. Starting with phase 15, the $R^2$ values of the filtered variants are significantly higher than those of the unfiltered variants. For the *RMSE* values, this is true for all phenological phases. Furthermore, it can be observed that the accuracy values improve with increasing vegetation development, which is related to the diminishing influence of the human factor and the increasing dominance of the temperature sum influence, respectively[12].

## Usage Notes

As a government research institution, the Julius Kühn Institute (JKI) operates a decentralized, cloud-integrated SDI to perform Big Data analyses of multi-hierarchical geospatial data time series[62]. The JKI SDI consists of three main components that are interoperably connected via standardized interfaces. The main components are the CODE-DE cloud platform for German authorities, which provides direct access to satellite imagery data and processing capabilities, and local JKI (geo)databases or storing vector, raster and metadata. The JKI Data Cube uses the rasdaman Array DBMS, and "gives access to multi-dimensional coverages via WMS for visualization, WCS for data extraction, reformatting, and download, and WCPS for safe server-side analytics"[63] (see Data Records section). The JKI Data Cube is composed of individual thematic cubes that can differ in terms of their spatial and temporal resolution and extent (Figure 7). In addition to the PHASE data cube with phase- and year-specific entry dates ($DOY^P$), three other Germany-wide Cubes were used for the usage notes. The DWD_TEMP_MAX and DWD_Niederschlag data cubes are characterized by a geometric resolution of $1 \times 1$ km$^2$, result from interpolated DWD station measurements, and contain daily maximum temperatures ($T^{d,max}$) and daily precipitation totals ($P^{d,sum}$), respectively, for the period from 1961 to the present. The S2_GermanyGrid_JKI data cube provides 10 cloud-masked atmospherically corrected spectral bands (*Blue*, *Green*, *Red*, *RedEdge*1, *RedEdge*2, *RedEdge*3, *NIR* 10 m, *NIR* 20 m, *SWIR*1, *SWIR*2) of the Sentinel-2 sensor for the entire area of Germany and the period from 2015 to present. While the S2_GermanyGrid_JKI data cubes are stored on the CODE-DE server in Frankfurt am Main, the other data cubes are located at the local JKI SDI in Braunschweig.

### WCS-based coupling of phenological, spectral information and weather data

A Jupyter notebook was created to query three different data cubes and obtain a common data set for a single winter wheat plot in Lower Saxony (Germany) in 2020[64]. In addition to the open PHASE data, multispectral Sentinel-2 imagery and precipitation data are also requested via WCS (Figure 7). The soil-adjusted vegetation index (*SAVI*)[65] is calculated from the Sentinel-2 data to provide information on canopy development throughout the growing season. Finally, a joint plot of all requested data is created (Figure 8).

| PLANT | PHASE | YEAR | ON | MSE | MAE | RMSE | R2 |
|---|---|---|---|---|---|---|---|
| 202 | 18 | 2021 | 326 | 14.6 | 3.09 | 3.82 | 0.38 |
| 202 | 18 | 2020 | 317 | 26.49 | 3.78 | 5.15 | 0.34 |
| 202 | 18 | 2019 | 342 | 21.85 | 3.74 | 4.67 | 0.41 |
| 202 | 18 | 2018 | 351 | 24.75 | 3.77 | 4.97 | 0.14 |
| 202 | 18 | 2017 | 411 | 14.93 | 3.18 | 3.86 | 0.46 |
| 202 | 18 | 2016 | 361 | 11.43 | 2.71 | 3.38 | 0.40 |
| 202 | 18 | 2015 | 355 | 26.41 | 4.02 | 5.14 | 0.39 |
| 202 | 18 | 2014 | 425 | 23.4 | 3.94 | 4.84 | 0.30 |
| 202 | 18 | 2013 | 500 | 22.35 | 3.44 | 4.73 | 0.48 |
| 202 | 18 | 2012 | 423 | 16.84 | 3.14 | 4.1 | 0.45 |
| 202 | 18 | 2011 | 516 | 17.3 | 3.38 | 4.16 | 0.57 |
| 202 | 18 | 2010 | 512 | 21.37 | 3.58 | 4.62 | 0.31 |
| 202 | 18 | 2009 | 567 | 16.68 | 3.24 | 4.08 | 0.39 |
| 202 | 18 | 2008 | 516 | 18.89 | 3.31 | 4.35 | 0.28 |
| 202 | 18 | 2007 | 451 | 24.09 | 3.90 | 4.91 | 0.36 |
| 202 | 18 | 2006 | 609 | 15.72 | 3.08 | 3.96 | 0.61 |
| 202 | 18 | 2005 | 625 | 23.87 | 3.73 | 4.89 | 0.47 |
| 202 | 18 | 2004 | 634 | 22.58 | 3.68 | 4.75 | 0.53 |
| 202 | 18 | 2003 | 634 | 14.05 | 3.04 | 3.75 | 0.46 |
| 202 | 18 | 2002 | 646 | 27.86 | 4.12 | 5.28 | 0.31 |
| 202 | 18 | 2001 | 563 | 31.08 | 4.34 | 5.57 | 0.32 |
| **202** | **18** | **2000** | **747** | **26.11** | **4.01** | **5.11** | **0.39** |
| 202 | 18 | 1999 | 851 | 19.58 | 3.52 | 4.42 | 0.36 |
| 202 | 18 | 1998 | 782 | 14.41 | 2.82 | 3.8 | 0.34 |
| 202 | 18 | 1997 | 972 | 21.53 | 3.59 | 4.64 | 0.38 |
| 202 | 18 | 1996 | 988 | 15.92 | 3.09 | 3.99 | 0.30 |
| 202 | 18 | 1995 | 991 | 32.01 | 4.39 | 5.66 | 0.44 |
| 202 | 18 | 1994 | 1083 | 28.57 | 4.14 | 5.34 | 0.37 |
| 202 | 18 | 1993 | 1025 | 20.82 | 3.56 | 4.56 | 0.36 |

**Table 7.** Global accuracy metrics of the interpolated optimal phenological observation variant for the winter wheat phase *heading* for the years 1993 to 2021 (PLANT — crop ID, PHASE -– phase ID, MAE – Mean Absolute Error, Mean Standard Error, RMSE – Root Mean Square Error, SN – observation sample number, R2 – Coefficient of determination).

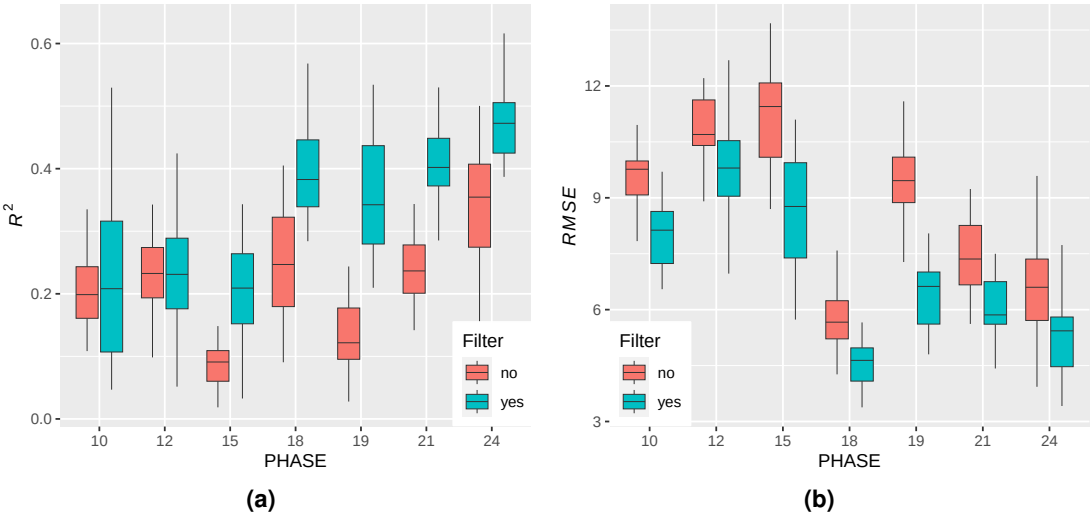


**Figure 6.** Comparison of phase-specific accuracy metrics Coefficient of determination ($R^2$) (a) and *RMSE* (b) for all interpolation results based on filtered and unfiltered phenological observations.

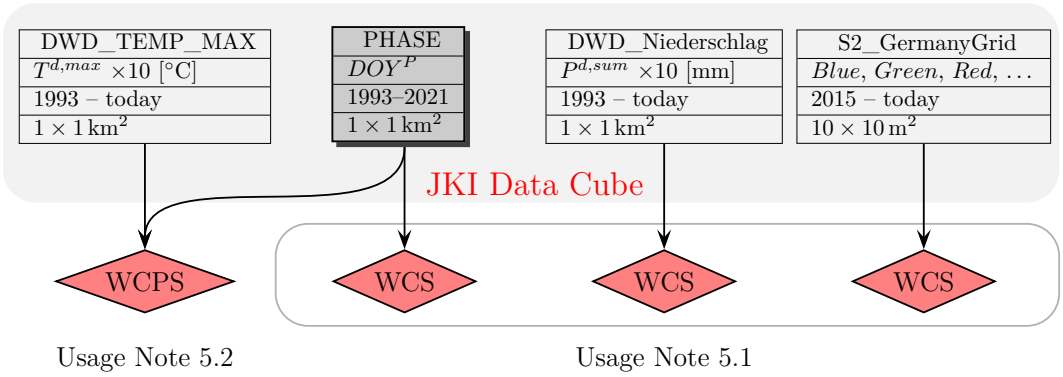


**Figure 7.** JKI data cube environment including the data cubes PHASE, DWD_TEMP_MAX, DWD_Niederschlag and S2_GermanyGrid.

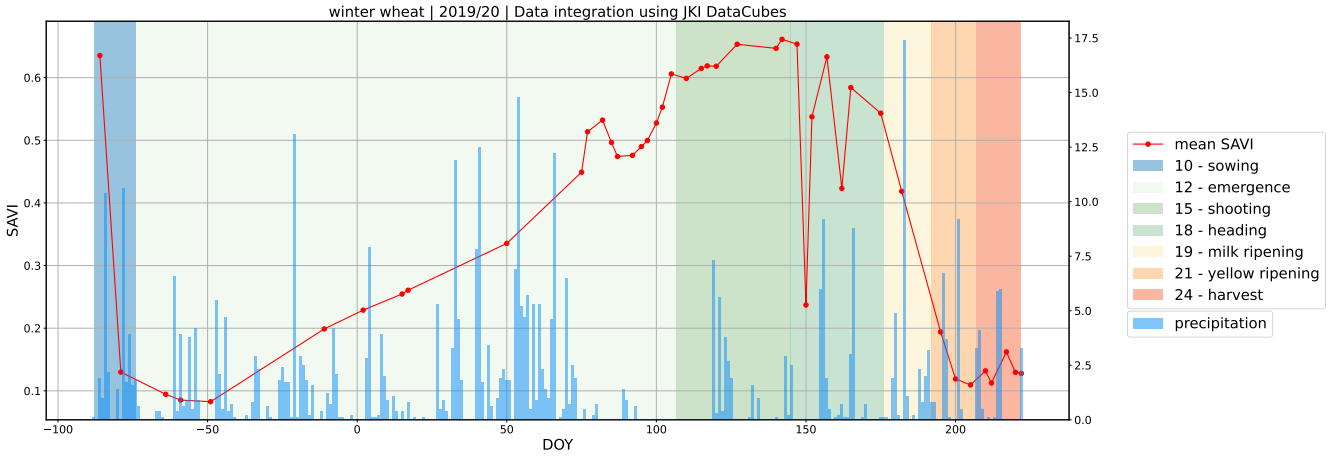


**Figure 8.** Coupling of data of different geometric and temporal resolution based on a WCS-based query using the example of phenological winter wheat phases (Table 6) and corresponding daily precipitation sums and *SAVI* time series within a parcel.

In the code example 3, the Python function `get_phases_from_point` is applied to determine the DOYs for the target winter wheat field in 2020. The function is stored in an additional Python file (`functions_DataCube.py`). Once the field boundaries are specified (*winterwheat2020.shp*), the function takes six mandatory parameters (target year, crop type, plot centroid coordinates, CRS of the field polygon, and the host address of the data cube) and two optional parameters (to get more information about the WCS request). The function creates a WCS-like URL with the specified parameters and performs the final query using the Python package `request`. If the query is successful, the function returns the received data in the form of a Python-like list containing all the initial dates of the phenological phases.

In the Jupyter notebook (`DemoPhaseWCS.ipynb`), we demonstrate how to run this function twice for the target year and the previous year (sowing and emergence of winter wheat), and two other functions for the additional data on the two other data cubes. Both the functions for PHASE data and precipitation data (`get_precipitation_from_point`) query only a single coordinate due to the coarse spatial resolution of $1 \times 1$ km$^2$. In contrast, the function for Sentinel-2 data (`get_tif_rasdaman`) queries an area of interest due to the spatial resolution of $10 \times 10$ m$^2$. The received spectral data are then averaged in further *SAVI* processing of the script.

## WCPS-based phase-specific temperature sums

While WCS allows the definition and download of spatio-temporal subsets of the multidimensional data cube (see Data Records section), an OGC-compliant WCPS can be used to integrate the data analysis into a query (see Data Records section). The analysis is performed directly on the data server, where the analysis results are also stored[66].

Code example 4 shows a WCPS statement for calculating phase-specific temperature totals. The query has been performed for an area near Braunschweig (Germany) for winter wheat phase 18 and the period between 06-10-1999 to 21-05-2000. The base temperature for winter wheat is 5.5°C. The temperature data is stored with a factor of 10, therefore the sum of

**Code example 3.** Quering PHASE Data Cube using WCS in Python

```python
import geopandas as gpd # python package to work with geovector data
from func_DataCube_PHASE import get_phases_from_point # import function from
    func_DataCube_PHASE.py
# directory to shape file of agricultural field'
shp = 'Vector/winterwheat2020.shp'
# get centroid coodinates from field and transform to CRS: 32632
easting = float(gpd.read_file(shp).to_crs('EPSG:32632').centroid.x)
northing = float(gpd.read_file(shp).to_crs('EPSG:32632').centroid.y)
# get phases from given year
year_on = '2020'
# wcs request:
phases_pre = get_phases_from_point(
    year=year_pre, # year
    crop='winterwheat', # crop type
    easting=easting, # longitude coordinate
    northing=northing, # latitude coordinagte
    epsg=32632, # crs of input and output
    host='https://datacube.julius-kuehn.de/flf/ows', # PHASE Data Cube web adress
    printout=False, # if True: information about request process are given
    get_query=True) # if True: prints the WCS query URL
print(phases_pre)

Output:
    https://datacube.julius-kuehn.de/flf/ows?&SERVICE=WCS&VERSION=2.0.1&REQUEST=GetCoverage&
        COVERAGEID=PHASE_202_Winterweizen&SUBSET=ansi("2020-01-01")&subsettingCrs=http://ows
        .rasdaman.org/def/crs/EPSG/0/32632&SUBSET=E(595342.5636430825,595342.5636430825)&
        SUBSET=N(5784876.418276947,5784876.418276947)&outputCrs=http://ows.rasdaman.org/def/
        crs/EPSG/0/32632&FORMAT=text/csv
    [106.6466, 144.8433, 175.9788, 192.0013, 206.8396, 281.4659, 292.5806]
```

**Code example 4.** WCPS query

```
for $tMin in (DWD_Temp_Min), $tMax in (DWD_Temp_Max)
let $t:= [ansi("1999-279":"2000-142")], $p:=[E(3598044), N(5797122)],
$cutout_tmin := $tMin[$t][$p], $cutout_tmax := $tMax[$t][$p]

return encode((condense +
    over $d ansi(imageCrsDomain($cutout_tmin, ansi))
    using( switch case
        (($cutout_tmin[ansi($d)] + $cutout_tmax[ansi($d)]) / 20.0 - 5.5  < 0.0)
            return 0.0
        default return
            ($cutout_tmin[ansi($d)] + $cutout_tmax[ansi($d)]) / 20.0 - 5.5
)) , "csv" )
```

| PHASE ID | PHASE name | PHASE start | PHASE end | temperature sum |
|---|---|---|---|---|
| 10 | Beginning of sowing | 1999-279 | 2000-275 | 1966.6 |
| 12 | Emergence | 1999-279 | 1999-292 | 53.4 |
| 15 | Beginning of shooting | 1999-279 | 2000-112 | 267.9 |
| **18** | **Beginning of heading** | **1999-279** | **2000-142** | **574.55** |
| 19 | Beginning of milk ripening | 1999-279 | 2000-172 | 885.7 |
| 21 | Beginning of yellow ripening | 1999-279 | 2000-198 | 1138.0 |
| 24 | Harvest | 1999-279 | 2000-218 | 1363.7 |

**Table 8.** Results of WCPS temperature sums queries for a location near Braunschweig and the year 2000 (see code example 4).

the daily maximum temperature and daily minimum temperature must be divided by 20 to obtain the correct average value. To simplify the query, the day length is left out. The determined temperature sum is 574.55°C. In Table 8, the temperature sums of the other phases are listed. Note that the growing season of winter crops starts in the year of sowing, here in 1999. The WCPS statement can also be translated into an URL statement with the following structure https://datacube.julius-kuehn.de/flf/ows?service=WCS&version=2.0.1&request=ProcessCoverages&query=<WCPS>[1].

## Code availability

All **R** functions of the PHASE model are located in the software repository[11] and can be executed by calling the wrapper file PhaseR.R. In addition, the wrapper file is explained in detail in a corresponding quarto® report[67].

## References


1. Schmidt, G., Schönrock, S. & Schröder, W. *Plant Phenology as a Biomonitor for Climate Change in Germany*. SpringerBriefs in Environmental Science (Springer International Publishing, Cham, 2014).
2. Schwartz, M. D., Kratochwil, A. & Lieth, H. *Phenology: An Integrative Environmental Science*, vol. 39 of *Tasks for Vegetation Science* (Springer Netherlands, Dordrecht, 2003).
3. Koch, E. Global Framework for Data Collection – Data Bases, Data Availability, Future Networks, Online Databases. In Hudson, I. L. & Keatley, M. R. (eds.) *Phenological Research – Methods for Environmental and Climate Change Analysis*, 23–61 (Springer, Dordrecht, Heidelberg, London, New York, 2010).
4. Kaspar, F., Zimmermann, K. & Polte-Rudolf, C. An overview of the phenological observation network and the phenological database of germany's national meteorological service (deutscher wetterdienst). *Adv. Sci. Res.* **11**, 93–99, 10.5194/asr-11-93-2014 (2014).
5. Meier, U. Growth stages of mono- and dicotyledonous plants: BBCH Monograph. 10.5073/20180906-074619 (2018). Publisher: Open Agrar Repositorium.
6. Bruns, E. *et al.* Vorschriften und Betriebsunterlagen für die phänologischen Beobachter des deutschen Wetterdienstes. Tech. Rep. 17, Deutscher Wetterdienst, Offenbach, Germany (2015).
7. Mehdipoor, H., Zurita-Milla, R., Rosemartin, A., Gerst, K. L. & Weltzin, J. F. Developing a Workflow to Identify Inconsistencies in Volunteered Geographic Information: A Phenological Case Study. *PLOS ONE* **10**, e0140811, 10.1371/journal.pone.0140811 (2015).
8. Senaratne, H., Mobasheri, A., Ali, A. L., Capineri, C. & Haklay, M. M. A review of volunteered geographic information quality assessment methods. *Int. J. Geogr. Inf. Sci.* **31**, 139–167, 10.1080/13658816.2016.1189556 (2017).
9. Dalhaus, T. & Finger, R. Can Gridded Precipitation Data and Phenological Observations Reduce Basis Risk of Weather Index–Based Insurance? *Weather. Clim. Soc.* **8**, 409–419, 10.1175/WCAS-D-16-0020.1 (2016).
10. Möller, M., Doms, J., Gerstmann, H. & Feike, T. A framework for standardized calculation of weather indices in Germany. *Theor. Appl. Climatol.* **136**, 377–390, 10.1007/s00704-018-2473-x (2019).
11. Möller, M. & Gerstmann, H. JKI-GDM/PhaseR: v1.0. *Zenodo* https://zenodo.org/badge/DOI/10.5281/zenodo.7867446.svg (2023).
12. Gerstmann, H., Doktor, D., Gläßer, C. & Möller, M. PHASE: A geostatistical model for the Kriging-based spatial prediction of crop phenology using public phenological and climatological observations. *Comput. Electron. Agric.* **127**, 726–738, 10.1016/j.compag.2016.07.032 (2016).
13. Möller, M., Boutarfa, L. & Strassemeyer, J. PhenoWin – An R Shiny application for visualization and extraction of phenological windows in Germany. *Comput. Electron. Agric.* **175**, 105534, 10.1016/j.compag.2020.105534 (2020).
14. Möller, M., Gerstmann, H., Gao, F., Dahms, T. C. & Förster, M. Coupling of phenological information and simulated vegetation index time series: Limitations and potentials for the assessment and monitoring of soil erosion risk. *CATENA* **150**, 192–205, 10.1016/j.catena.2016.11.016 (2017).
15. Strassemeyer, J., Daehmlow, D., Dominic, A., Lorenz, S. & Golla, B. SYNOPS-WEB, an online tool for environmental risk assessment to evaluate pesticide strategies on field level. *Crop. Prot.* **97**, 28–44, 10.1016/j.cropro.2016.11.036 (2017).


[1]The hyperlink contains the complete query.

**16.** Gerstmann, H., Gläßer, C., Thürkow, D. & Möller, M. Detection of phenology-defined data acquisition time frames for crop type mapping. *PFG – J. Photogramm. Remote. Sens. Geoinformation Sci.* **86**, 15–27, 10.1007/s41064-018-0043-6 (2018).

**17.** Duden, C., Urban, J., Offermann, F., Hirschauer, N. & Möller, M. Die Wirkung von Ertrags- und Wetterindexversicherungen auf das Erfolgsrisiko deutscher Ackerbaubetriebe - wird die Hedgingeffektivität überschätzt? *Berichte über Landwirtschaft* **97**, 1–39 (2019).

**18.** Abdi, A. M. *et al.* Biodiversity decline with increasing crop productivity in agricultural fields revealed by satellite remote sensing. *Ecol. Indic.* **130**, 108098, 10.1016/j.ecolind.2021.108098 (2021).

**19.** Bucheli, J., Dalhaus, T. & Finger, R. Temperature effects on crop yields in heat index insurance. *Food Policy* **107**, 102214, 10.1016/j.foodpol.2021.102214 (2022).

**20.** Riedesel, L. *et al.* Timing and Intensity of Heat and Drought Stress Determine Wheat Yield Losses in Germany. *SSRN Electron. J.* 10.2139/ssrn.4243420 (2022).

**21.** Marrec, R., Brusse, T. & Caro, G. Biodiversity-friendly agricultural landscapes – integrating farming practices and spatiotemporal dynamics. *Trends Ecol. & Evol.* **37**, 731–733, 10.1016/j.tree.2022.05.004 (2022).

**22.** DOI Foundation. Digital Object Identifier, https://www.doi.org (2023). Accessed 23-March-2023.

**23.** Wilkinson, M. D. *et al.* The FAIR Guiding Principles for scientific data management and stewardship. *Sci. Data* **3**, 10.1038/sdata.2016.18 (2016).

**24.** Senft, M., Stahl, U. & Svoboda, N. Research data management in agricultural sciences in Germany: We are not yet where we want to be. *PLOS ONE* **17**, e0274677, 10.1371/journal.pone.0274677 (2022).

**25.** Wagemann, J., Clements, O., Marco Figuera, R., Rossi, A. P. & Mantovani, S. Geospatial web services pave new ways for server-based on-demand access and processing of Big Earth Data. *Int. J. Digit. Earth* **11**, 7–25, 10.1080/17538947.2017.1351583 (2018).

**26.** Lacayo, M., Rodila, D., Giuliani, G. & Lehmann, A. A framework for ecosystem service assessment using GIS interoperability standards. *Comput. & Geosci.* **154**, 104821, 10.1016/j.cageo.2021.104821 (2021).

**27.** Reinecke, R., Trautmann, T., Wagener, T. & Schüler, K. The critical need to foster computational reproducibility. *Environ. Res. Lett.* **17**, 041005, 10.1088/1748-9326/ac5cf8 (2022).

**28.** Team, R. C. *R: A Language and Environment for Statistical Computing* (R Foundation for Statistical Computing, Vienna, Austria, 2021).

**29.** Ahmad, L., Habib Kanth, R., Parvaze, S. & Sheraz Mahdi, S. Growing Degree Days to Forecast Crop Stages. In *Experimental Agrometeorology: A Practical Manual*, 95–98, 10.1007/978-3-319-69185-5_14 (Springer International Publishing, Cham, 2017).

**30.** Zhou, G. & Wang, Q. A new nonlinear method for calculating growing degree days. *Sci. Reports* **8**, 10149, 10.1038/s41598-018-28392-z (2018).

**31.** Hengl, T., Heuvelink, G. B. & Rossiter, D. G. About regression-kriging: From equations to case studies. *Comput. & Geosci.* **33**, 1301–1315, 10.1016/j.cageo.2007.05.001 (2007).

**32.** Li, J. & Heap, A. D. Spatial interpolation methods applied in the environmental sciences: A review. *Environ. Model. & Softw.* **53**, 173–189, 10.1016/j.envsoft.2013.12.008 (2014).

**33.** Dekking, F. M., Kraaikamp, C., Lopuhaä, H. P. & Meester, L. E. *A Modern Introduction to Probability and Statistics*. Springer Texts in Statistics (Springer London, London, 2005).

**34.** Janssen, W. *Beschreibung des Interpolationsverfahrens* (Deutscher Wetterdienst, Abteilung Agrarmeteorologie, Offenbach, 2009).

**35.** Wikipedia. Pearson correlation coefficient, https://en.wikipedia.org/wiki/Pearson_correlation_coefficient (2023). Accessed 23-March-2023.

**36.** Wikipedia. Root-mean-square deviation, https://en.wikipedia.org/wiki/Root-mean-square_deviation (2023). Accessed 23-March-2023.

**37.** Wikipedia. Mean absolute error, https://en.wikipedia.org/wiki/Mean_absolute_error (2023). Accessed 23-March-2023.

**38.** Wood, S. N. Thin plate regression splines: *Thin Plate Regression Splines. J. Royal Stat. Soc. Ser. B (Statistical Methodol.* **65**, 95–114, 10.1111/1467-9868.00374 (2003).

**39.** Hiemstra, P. H., Pebesma, E. J., Twenhöfel, C. J. & Heuvelink, G. B. Real-time automatic interpolation of ambient gamma dose rates from the Dutch radioactivity monitoring network. *Comput. & Geosci.* **35**, 1711–1721, 10.1016/j.cageo.2008.10.011 (2009).

**40.** Nychka, D., Furrer, R., Paige, J. & Sain, S. fields: Tools for spatial data. *The Compr. R Arch. Netw. CRAN* https://github.com/dnychka/fieldsRPackage (2021).

**41.** Meyer, H. & Pebesma, E. Machine learning-based global maps of ecological variables and the challenge of assessing them. *Nat. Commun.* **13**, 2208, 10.1038/s41467-022-29838-9 (2022).

**42.** Specka, X. *et al.* The BonaRes metadata schema for geospatial soil-agricultural research data – Merging INSPIRE and DataCite metadata schemes. *Comput. & Geosci.* **132**, 33–41, 10.1016/j.cageo.2019.07.005 (2019).

**43.** DataCite. Datacite – connecting research, advancing knowledge, https://datacite.org/ (2023). Accessed 23-March-2023.

**44.** European Commission. INSPIRE – infrastructure for spatial information in Europe, https://inspire.ec.europa.eu/ (2023). Accessed 23-March-2023.

**45.** Food and Agriculture Organization (FAO). AGROVOC – linked open data set about agriculture, https://www.fao.org/agrovoc/ (2023). Accessed 23-March-2023.

**46.** European Environment Agency (EEA). GEMET – GEneral Multilingual Environmental Thesaurus, https://www.eionet.europa.eu/gemet (2023). Accessed 23-March-2023.

**47.** Creative Commons Network. Creative Commons, https://de.creativecommons.net/ (2023). Accessed 23-March-2023.

**48.** Möller, M., Gerstmann, H. & Horney, P. Germany-wide time series of interpolated phenological observations for main crop types between 1993 and 2021, BONARES-JE6G-9896. Type: dataset.

**49.** Rauthe, M., Steiner, H., Riediger, U., Mazurkiewicz, A. & Gratzki, A. A Central European precipitation climatology Part I: Generation and validation of a high-resolution gridded daily data set (HYRAS). *Meteorol. Zeitschrift* **22**, 235–256, 10.1127/0941-2948/2013/0436 (2013). Place: Stuttgart, Germany Publisher: Schweizerbart Science Publishers.

**50.** Kaspar, F., Kratzenstein, F. & Kaiser-Weiss, A. K. Interactive open access to climate observations from Germany. *Adv. Sci. Res.* **16**, 75–83, 10.5194/asr-16-75-2019 (2019).

**51.** Open Geospatial Consortium (OGC). Web Coverage Service (WCS), https://www.ogc.org/standard/wcs/ (2023). Accessed 23-March-2023.

**52.** Open Geospatial Consortium (OGC). Web Mapping Service (WMS), https://www.ogc.org/standard/wms/ (2023). Accessed 23-March-2023.

**53.** Julius Kühn Institute (JKI). Phase Data Cube Web Coverage Service (PHASE WCS), https://sf.julius-kuehn.de/openapi/phase/ (2023). Accessed 23-March-2023.

**54.** Baumann, P., Misev, D., Merticariu, V. & Huu, B. P. Array databases: concepts, standards, implementations. *J. Big Data* **8**, 28, 10.1186/s40537-020-00399-2 (2021).

**55.** Baumann, P. & Escriu, J. INSPIRE coverages: an analysis and some suggestions. *Open Geospatial Data, Softw. Standards* **4**, 1, 10.1186/s40965-019-0059-x (2019).

**56.** Open Geospatial Consortium (OGC). Web Coverage Processing Service (WCPS), https://www.ogc.org/standard/wcps/ (2023). Accessed 23-March-2023.

**57.** The ogc web coverage processing service (wcps) standard. .

**58.** Thas, O. *Comparing distributions*. Springer series in statistics (Springer). OCLC: ocn401153891.

**59.** Khaledian, Y. & Miller, B. A. Selecting appropriate machine learning methods for digital soil mapping. **81**, 401–418, 10.1016/j.apm.2019.12.016.

**60.** Wikipedia. Mean squared error, https://en.wikipedia.org/wiki/Mean_squared_error (2023). Accessed 23-March-2023.

**61.** Wikipedia. Coefficient of determination, https://en.wikipedia.org/wiki/Coefficient_of_determination (2023). Accessed 23-March-2023,.

**62.** Beyer, F. *et al.* A paradigm shift towards decentralized cloud-integrated spatial data infrastructures: Lessons learned and solutions provided for public authorities. (2023). Submitted.

**63.** Baumann, P. A general conceptual framework for multi-dimensional spatio-temporal data sets. *Environ. Model. & Softw.* **143**, 105096, 10.1016/J.ENVSOFT.2021.105096 (2021).

**64.** Beyer, F. JKI-GDM/DemoPhaseWCS: v1.0, 10.5281/ZENODO.7893966.

**65.** Huete, A. A soil-adjusted vegetation index (SAVI). *Remote. Sens. Environ.* **25**, 295–309, 10.1016/0034-4257(88)90106-X (1988).

**66.** Baumann, P. The OGC web coverage processing service (WCPS) standard. **14**, 447–479, 10.1007/s10707-009-0087-2.

**67.** Möller, M. PhaseR – R functions to download, filter and interpolate phenological observations. *Rpubs* https://doi.org/10.5073/20230411-094013-0 (2023).

## Acknowledgements

The study was created by financial support of the projects and initiatives: NFDI Consortium FAIRagro funded by Deutsche Forschungsgemeinschaft (DFG – German Research Foundation; project number 501899475), MonViA funded by the German Federal Ministry of Food and Agriculture, NaLamKI funded by the Federal Ministry of Economic Affairs and Climate Action (contract no. 01MK21003E) as well as DynAWI funded by the German Federal Ministry of Food and Agriculture (contract no. 28DK118A20). We thank the DWD for providing interpolated precipitaion and temperature data.

## Author contributions statement

M.M. was the lead author, created the dataset, adapted the PHASE model, documented the model and dataset on Github, Rpubs and Zenodo, and wrote the original draft. The original model was developed by H.G. who also contributed to the model description in the manuscript. Supported by P.B., M.D. and P.B. created, curated, described and documented both types of web services (WCS, WCPS). Together with F.B., M.D. also created an usage note. N.S. described the Bonares Repository. P.H. provided model input data. All authors reviewed the manuscript.

## Competing interests

The authors declare no competing interests.

## Acronyms

*COR* Pearson correlation coefficient. 7

*MAE* Mean Absolute Error. 7, 12

*MSE* Mean Squared Error. 12

*RMSE* Root Mean Squared Error. 7, 12, 13

$R^2$ Coefficient of determination. 12, 13

**ARTS** analysis-ready time series. 2, 11

**DOI** Digital Object Identifier. 2, 10

**DOY** Day(s) of the Year. 2, 4–7, 9, 11, 14

**DWD** German Meteorological Service. 1, 2, 5, 6, 11, 12, 19

**GDD** Growing Degree Days. 2

**GIS** geographic information system. 11

**JKI** Julius Kühn Institute. 12

**OGC** Open Geospatial Consortium. 11, 14

**RDM** Research Data Management. 7, 10

**SDI** Spatial Data Infrastructure. 7, 10, 12

**VGI** volunteered geographical information. 1

**WCPS** Web Coverage Processing Service. 11, 12, 14–16

**WCS** Web Coverage Service. 2, 11, 12, 14, 15

**WMS** Web Map Service. 7, 11, 12